

# Dynamic Functional Network Analysis in Mild Traumatic Brain Injury

Wenshuai Hou,<sup>1</sup> Chandler Sours Rhodes,<sup>2</sup> Li Jiang,<sup>2</sup> Steven Roys,<sup>2</sup>  
Jiachen Zhuo,<sup>2</sup> Joseph JaJa,<sup>1</sup> and Rao P. Gullapalli<sup>2</sup>

## Abstract

Mild traumatic brain injury (mTBI) is one of the most common neurological disorders for which a subset of patients develops persistent postconcussive symptoms. Previous studies discovered abnormalities and disruptions in the brain functional networks of mTBI patients principally using static functional connectivity measures which assume that neural communication across the brain is static during resting state conditions. In this study, we examine the differences in dynamic neural communication between mTBI and control participants through the application of a combination of dynamic functional analysis and graph theoretic algorithms. Resting state functional magnetic resonance imaging data was obtained on 47 mTBI patients at the acute stage of injury and 30 demographically matched healthy control participants. Results show unique alterations in both the static and dynamic functional connectivity at the acute stage in mTBI patients who suffer persistent symptoms ( $\geq 6$  months after injury). In addition, mTBI patients with postconcussion syndrome demonstrated a unique allocation of time in various brain states compared to both control participants and mTBI patients with favorable outcomes. These findings suggest that global damage to the overall communication across the brain in the acute stage may contribute to chronic mTBI symptoms. Dynamic functional analysis is a powerful tool that provides insights into the brain states and the innovative analysis methodology utilized may hold the potential to delineate patients predisposed to poor outcomes upon early presentation following injury.

**Keywords:** dynamic functional connectivity; graph theory; mild traumatic brain injury; postconcussive syndrome

## Introduction

**T**RAUMATIC BRAIN INJURY (TBI) is one of the most common neurological disorders in the United States with  $\sim 1.5$  million cases reported annually (Faul et al., 2010). The vast majority of these cases ( $\sim 75\%$ ) are diagnosed as mild TBI (mTBI) based on a Glasgow Coma Scale (GCS) score of 13–15. Many patients seek treatment in the emergency room but because conventional magnetic resonance imaging (MRI) and computed tomography (CT) often lack the sensitivity to detect subtle intracranial injuries in mTBI patients, these patients are immediately discharged and rarely receive follow up care for their injury. Although many patients diagnosed with mTBI make a full recovery in the first weeks after injury, a significant subset develops persistent postconcussion syndrome (PCS) (McMahon et al., 2014). These symptoms include cognitive deficits, somatic complaints, and neuropsychological symptoms (Dischinger et al., 2009).

The lack of suitable biological or imaging markers in the acute stage of injury to indicate long-term prognosis remains a considerable challenge facing clinicians. Therefore, further research on early diagnosis and outcome prediction is needed to distinguish which patients may have the propensity for a poor outcome following mTBI, ultimately allowing for early interventions to mitigate chronic symptoms.

Numerous studies have focused on understanding disruptions within specific neural networks and have noted alterations in resting state functional connectivity following mTBI across multiple stages of injury (Mayer et al., 2011; Sours et al., 2013, 2015b; Stevens et al., 2012; Tang et al., 2011; Vergara et al., 2017b; Zhou et al., 2012). However, considering the heterogeneous nature of the initial impact and the variable nature of the diffuse damage with potential for proliferation toward secondary injury mechanisms associated with mTBI, network level properties that assess global functional communication may be more sensitive to frequently

<sup>1</sup>Department of Electrical and Computer Engineering, University of Maryland Institute for Advanced Computer Services (UMIACS), College Park, Maryland.

<sup>2</sup>Department of Diagnostic Radiology and Nuclear Medicine, University of Maryland School of Medicine, Baltimore, Maryland.

subtle focal injuries. Furthermore, traditional resting state functional connectivity analysis makes the assumption that the neural communication across the brain is stable during resting state conditions. Yet, even during so-called “resting state,” it is known that an individual’s mind wanders and that this dynamic process results in great variability in the patterns of functional communication over time (Chang and Glover, 2010). Recent advances in the field have shown that additional information regarding anomalies in neural network communication can be extracted from the dynamic nature of functional connectivity (Calhoun et al., 2014; Hutchison et al., 2013). This additional information may provide complementary insights to those obtained from static functional connectivity analysis.

While the majority of groups that investigated functional connectivity following mTBI have used static functional connectivity analysis, recently, groups have started to consider how dynamic changes in functional connectivity may be altered following mTBI (Mayer et al., 2015; Vergara et al., 2017a; Vergara et al., 2017b; Vergara et al., 2018) as well as moderate and severe TBI (Gilbert et al., 2018). In spite of differences in methodology, these groups have presented variable levels of success in using dynamic functional connectivity measures, either globally or within individual sub-networks, to both characterize and discriminate TBI populations from control groups. However, these studies have investigated dynamic connectivity metrics at various stages of injury, have been limited to a single time point, and have not considered long-term outcomes of the patients in the analysis. Hence, no comparisons were made between patients with good and poor outcomes, based on either current symptomology or future, persistent symptoms.

We hypothesize that the static and dynamic networks differ significantly between patients who have poor outcomes compared to those patients who make full recoveries. We explored this idea by using a data-driven method that does not make any prior assumptions about the pathology of mTBI to determine if network level properties of dynamic functional connectivity present during the acute stage of injury provide unique information regarding temporal dynamics of neural

communication. Furthermore, we investigated whether these measures have the ability to detect differences between mTBI subjects who fully recover and those who suffer from persistent PCS.

## Materials and Methods

### Participants

Forty-seven mTBI patients ( $41.7 \pm 17.3$  years, 34 M/13 F) were prospectively recruited from the R Adams Cowley Shock Trauma Center at the University of Maryland Medical Center as part of a larger protocol using a combination of advanced MRI and neuropsychological assessments. This study was approved by the University of Maryland institutional review board. All mTBI patients were scanned within 10 days of injury (range: 0–10 days; mean: 7 days). Thirty neurologically intact subjects ( $40.2 \pm 18.4$  years, 18 M/12 F) served as the control population. All participants were over the age of 18. Control and mTBI participants were excluded for history of neurological or psychiatric disorder, history of stroke, seizures, brain tumors, or previous brain injury requiring hospitalization. Patients were classified into the mTBI category if they had an admission GCS of 13–15 and a mechanism of injury consistent with trauma. In addition, mTBI patients were included based on either (1) positive head CT or (2) loss of consciousness and/or amnesia and evidence of head trauma consistent with TBI. Based on the inclusion criteria, this study included patients classified as complicated mTBI (positive admission head CT) and uncomplicated mTBI (negative admission head CT). It is important to note, that those patients we have classified as complicated mTBI may be categorized as moderate TBI based upon other classification systems such as the Department of Defense/Veteran Affairs or Mayo TBI classification systems. Mechanisms of injury included falls, motor vehicle accidents, motorcycle accidents, accidental hits with blunt objects, assaults, bicycle accidents, and recreational sports accidents (see Table 1 for breakdown of injury mechanisms between groups).

The mTBI population was further divided into two cohorts including those with PCS (PCS+) and those without PCS

TABLE 1. DEMOGRAPHICS

	HC	PCS+	PCS–	Statistical difference
<i>n</i>	30	24	23	
Age	40.2 ± 18.4	44.5 ± 17.5	38.8 ± 16.9	$F = 0.696$ ; $p = 0.50$
Education	15 ± 2	14 ± 2	14 ± 3	$F = 1.927$ ; $p = 0.15$
Sex	18 M/12 F	15 M/9 F	19 M/4 F	$\chi^2 = 3.4$ ; $p = 0.18$
GCS	NA	14.6 ± 0.7	15.0 ± 0.2	$p = 0.04$
Days postinjury	NA	7 ± 3	6 ± 3	$p = 0.49$
MR+ or CT+	NA	8/24 (33%)	7/23 (30%)	
Mechanism of injury				
MCC	NA	4 (16%)	2 (9%)	
MVC	NA	5 (21%)	2 (9%)	
Fall	NA	11 (46%)	8 (35%)	
Bicycle	NA	2 (8%)	2 (9%)	
Sports accident	NA	0 (0%)	2 (9%)	
Hit with blunt object	NA	1 (4%)	2 (9%)	
Assault	NA	1 (4%)	5 (22%)	

Demographics of the three groups including the healthy control population and the TBI population consisting of PCS+ and PCS–.

CT, computed tomography; GCS, Glasgow Coma Scale; HC, healthy controls; MR, magnetic resonance; NA, not applicable; PCS, post-concussion syndrome; PCS+, patients with PCS; PCS–, patients without PCS; MCC, motorcycle collision; MVC, motor vehicle collision.

(PCS-) based on self-reported symptoms on the Modified Rivermead Post Concussion Questionnaire (RPQ) at a 6 month follow-up visit (King et al., 1995). The RPQ asks participants to rate a series of common postconcussive symptoms on a scale of 0–4. Based on the International Classification of Disease 10th revision (ICD10) symptom criteria for PCS, PCS was defined as those who reported three or more of the following symptoms lasting for greater than three months: sleep disturbances, headaches, dizziness, trouble concentrating, memory problems, fatigue, and irritability (World Health Organization, 2010).

#### Magnetic resonance data acquisition

All imaging was performed on a Siemens Tim-Trio 3T MRI scanner (Malvern, PA) using a 12-channel receive-only head coil. A high-resolution T1-weighted magnetization prepared rapid acquisition gradient echo (T1-MPRAGE) (echo time [TE] = 3.44 msec, repetition time [TR] = 2250 msec, inversion time [TI] = 900 msec, flip angle = 9°, resolution = 256 × 256 × 96, field-of-view [FOV] = 22 cm, slices thickness = 1.5 mm) was acquired for anatomic reference with slices parallel to the anterior and posterior commissure points. For the resting state functional MRI (fMRI) scan, T2\*-weighted images were acquired using a single-shot echoplanar imaging sequence (TE = 30 msec, TR = 2000 msec, FOV = 230 mm, resolution = 64 × 64) with 36 axial slices (slices thickness = 4 mm) over 5 min 42 sec that yielded 171 volumes after discarding the first three volumes to minimize steady state effects. During the resting state scans, the participants were instructed to rest peacefully with their eyes closed.

#### fMRI data preprocessing

Standard preprocessing steps were applied to the resting state fMRI data using AFNI (Cox, 1996). Preprocessing included slice timing correction, registration of all 171 volumes to the first volume of the time series, normalization to percent signal change, spatial smoothing (6 mm Gaussian Kernel), and band pass filtering ( $0.005 \text{ Hz} < f < 0.1 \text{ Hz}$ ). The structural T1-MPRAGE was co-registered to the resting state mean blood oxygenation level dependent (BOLD) data and segmented to white matter (WM), gray matter and cerebrospinal fluid (CSF) using SPM8 (SPM8, 2009). The average signal from the mean BOLD time series from the WM and CSF mask and the six motion correction parameters were included in the model as regressors to remove the variance related to non-neuronal contributions and motion. Resting state BOLD data was spatially normalized to Talairach space using the transformation matrix from the registration of the T1-MPRAGE to the TT\_N27 Talairach template within AFNI (Talairach and Tournoux, 1988). Resting state BOLD data was spatially resampled to 2mm isotropic resolution.

#### Network analysis methodology

The processing pipeline used in this study is illustrated in Figure 1. The first step consists of a group-level independent component analysis (ICA) that was applied to the resting state fMRI data for all the subjects to generate a common set of nonoverlapping spatial patterns. A hierarchical model was used to extract these common spatial patterns based on the canonical ICA (canICA) as discussed below. Subject specific time courses corresponding to each spatial

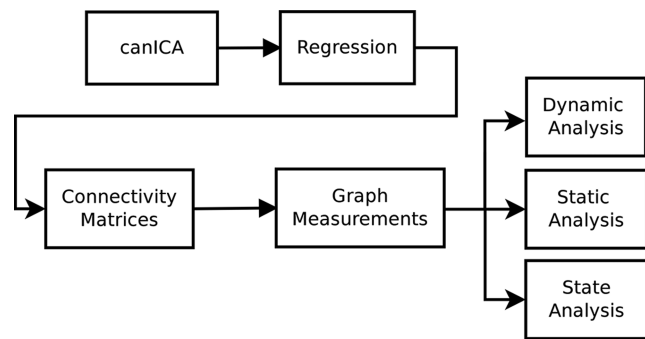


**FIG. 1.** Diagram outlining the analysis pipeline. canICA, canonical independent component analysis.

pattern were reconstructed using the robust Ridge regression method (Hoerl and Kennard, 1970; Pedregosa et al., 2011). Finally, for each subject, a series of functional connectivity weighted graphs were constructed, capturing the functional interactions during a sliding time window. The sliding window consists of 28 temporal overlapping epochs, with a step length of 5 time points (10 sec). Various window sizes and step lengths were investigated with similar results (Supplementary Tables S1–S4). These graphs were then used to investigate graph properties of the functional networks on an individual basis.

Graph properties investigated include the average shortest path (SP), average clustering coefficient (CC), and average weight of the minimum spanning trees (MST). Group differences in the neural communication properties among the three population groups were examined in two different ways. First, *global functional network analysis* was completed. For each subject, the temporal dynamics of the global functional network were determined by computing the moving pair-wise absolute difference between network properties of adjacent time windows using all the independent components. Second, a *state analysis* was used to identify typical functional network states, followed by investigation of the characteristics of each state and the distribution of time spent in each state by subjects of the different groups. Such analysis enabled us to shed more light on the differences among the three groups. In addition, preliminary analysis was performed to investigate alterations in static and dynamic connectivity within various sub-networks. For each subject and for a given set of sub-networks, the temporal dynamics of each individual sub-network were determined by computing the pair-wise absolute difference between network properties of adjacent time windows using only components within the given sub-network.

#### Group level spatial patterns and subject-specific time courses

We used canICA to generate group level spatial maps (Varoquaux et al., 2010a, 2010b). The canICA processing pipeline determines a set of spatial map components that are common to all subjects; this is performed through a hierarchical model with multiple stages of estimation and data processing. A detailed explanation of the mathematical methodologies behind this approach can be found in Varoquaux et al. (2010b) and is briefly described below.

canICA uses principal component analysis to project the data onto the subspace that captures most of the variance in the data. Specifically, singular value decomposition was used to decompose the observation matrix  $Y_s$  of each subject  $s$ , to determine the top components. Various numbers of components were investigated (20, 40, 50, 80, and 100) with similar results. The results represent the top 40 components, and are consistent and comparable with prior research (Sair et al., 2016; Tie et al., 2014; Varoquaux et al., 2010b). At a group level, canonical correlation analysis was used to find a common shared subspace that captures the maximum correlation among all the subjects and to identify a stable-component subspace. The FASTICA algorithm (Hyvarinen, 1999) was applied on this subspace to determine the group level independent components. These components provided group level spatial maps. FASTICA identified 40 spatial patterns of which 34 components were labeled with known functional regions and the remaining six were discarded as noise due to activation patterns within WM and CSF. The independent components thus determined were assigned to the following sub-networks: visual network, cognitive control network, default mode network (DMN), auditory network, cerebellar network, sub-cortical network, and sensorimotor network (Fig. 2). The labeling scheme is similar to what has been reported in the literature (van den Heuvel et al., 2009; Varoquaux et al., 2010b). This set of spatial patterns for these networks was used to make group comparisons among the three cohorts.

Subject-specific BOLD time series were derived from the resting state data for each of the 34 identified spatial components using the robust Ridge regression method with cross validation (Hoerl and Kennard, 1970; Pedregosa et al., 2011). The subject-specific time series were used to construct

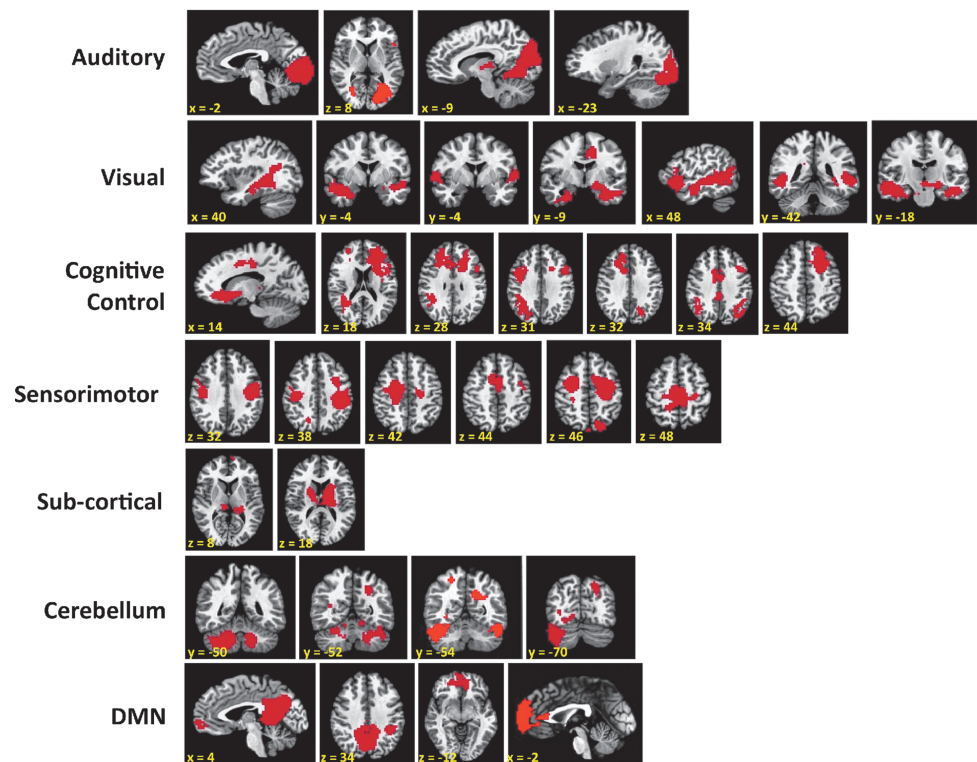
the functional network  $G=(V,E)$ , where  $V$  consists of 34 vertices corresponding to the 34 group level spatial patterns, and  $E$  consists of the edges between all pairs of vertices such that the weight of each edge is the distance between the two time series corresponding to the end points of the edge. We selected the L1 norm metric to capture the distance between the time series of spatial components, which is more appropriate than a similarity measure such as correlation for our graph-theoretic metrics. In many applications, the L1 norm has been used for the analysis and clustering of time series. The recent work of Ding et al. (2008) performs a thorough comparison between the various distance measures used to analyze time series, and shows that the L1 norm is a competitive distance metric comparable to the Euclidean and slightly inferior to the Dynamic Time Warping metric in some cases. Overall the L1 norm is considered to be a reliable measure of dissimilarity between two time series.

#### Functional network construction and network measurements

To measure different aspects of the dynamics of the functional networks, the following network characteristics were computed.

**Average SP.** This parameter, which is also referred to as the characteristic path length, is a measure of the global connectivity in the network and represents the efficiency of the information exchange on a network (Cherkassky et al., 1996). The algorithm is used to find the path that has smallest accumulative weight  $d(s,t)$  to travel from a vertex,  $s \in V$  to another vertex  $t \in V$  of a weighted graph. The average SP length is defined by:

**FIG. 2.** Visual representation of the component derived by canICA divided into seven functional sub-networks. They are labeled according to their anatomical positions: visual, auditory, cognitive control, sensorimotor, sub-cortical, cerebellum, and default mode network.



$$a = \sum_{(s,t) \in V} \frac{d(s,t)}{n(n-1)} \quad (1)$$

where  $|V|=n$ .

**Average local CC.** This parameter quantifies how close the neighbors of a vertex are to being a clique. In other words, it captures the level of local connectedness of the network. The networks with larger average CCs have a more modular structure than those with smaller average CCs (Watts and Strogatz, 1998). We use the weighted-graph variant of CC as defined in Saramaki et al. (2007). *The average clustering coefficient C is computed as:*

$$c_u = \frac{1}{deg(u)deg(u) - 1} \sum_{uv \in V} (\hat{e}_{uv}\hat{e}_{uw}\hat{e}_{vw})^{1/3} \quad (2)$$

$$c_u = \frac{1}{n} \sum_{u \in V} c_u \quad (3)$$

Where the edge weight  $\hat{e}_{uv}$  are normalized by maximum weight in the network:  $\hat{e}_{uv} = e_{uv}/max(e)$ , and  $deg(u)$  is the connectivity degree of vertex u, which is 34 in this work.

**Average weight of MST.** An MST is a sub-graph that contains all the vertices such that the sub-graph is a tree and the sum of the weights of its edges is at a minimum. The weight of a MST is used to estimate the minimal broadcast cost of the original graph (Pettie and Ramachandran, 2002).

*Sliding window analysis*

The most popular dynamic functional analysis method involves a sliding window of fixed size over the time domain. The entire time series of 171 time points was segmented into 28 overlapping short time intervals each a length of 28 TRs with a step size of 5 TRs. For each time window  $k$ , we define a distance matrix  $D^k$  of size  $34 \times 34$  which captures the dynamics between all pairs of spatial components during time window  $k$ . More specifically, for each subject, the  $(i, j)^{th}$  element of  $D^k$  is computed as the L1 norm between the time series  $X_i^k, X_j^k$  corresponding to components  $X_i$  and  $X_j$  over the  $k^{th}$  time window segment:

$$D_{ij}^k = d_j(X_i^k, X_j^k) \quad (4)$$

where  $d_j()$  is the sum of the absolute values of the differences between the corresponding elements of the time series. Each distance matrix defines a weighted adjacency matrix of the functional network corresponding to the same time window.

The above mentioned graph theoretic parameters were computed for each functional network defined over a time window. Therefore, each subject in this study was characterized by a series of scores. For example, the series of the average SP for subject,  $s$ , can be denoted by:  $Z_s = \{z_{s,k}, k=1, \dots, K\}$ , where  $z_{s,k}$  is the average SP of the subject  $s$ ' network defined over the time window  $k$ , and  $K$  is the number of window segments.

*Static connectivity*

For each subject, we computed the static functional connectivity of the time series of each type (SP, CC, MST) of

network measurements as shown in Equation (5). For each subject  $s$ , a static functional connectivity network is constructed using the L1 norm between the individual's time series. The L1 norm between time series  $X_i$  and time series  $X_j$  is computed as shown in Equation (5).

$$D_{ij,s,static} = \sum_{p=1}^{171} |X_i^p - X_j^p| \quad (5)$$

where  $X_i^p$  is the  $p^{th}$  time point of the  $j^{th}$  time series of subject  $s$ .

The three types of network measurements as described above were performed on the static functional connectivity network, producing  $Z_{SP,s,static}$ ,  $Z_{MST,s,static}$ , and  $Z_{CC,s,static}$ .

*Dynamic connectivity*

The dynamic aspects of the network measurement can be captured by using the average of the scaled differences of the scores between consecutive values as described in Equation (6) for SP.

$$Z_{SP,s,dynamic} = \frac{1}{K-1} \sum_{k=1}^{K-1} \left| \frac{z_{SP,s,k+1} - z_{SP,s,k}}{z_{SP,s,k}} \right| \quad (6)$$

The normalization in the denominator is necessary to correct the effect of the magnitudes of the values appearing in the original time series. The more dynamic or variable the functional states are, the larger this summary score will be.

*Statistical analysis*

For each network measurement, each subject was characterized by a series of static and dynamic scores for each of SP, CC, and MST respectively. Analysis of variance (ANOVA) was performed to detect possible group level differences. For the measurements with a significant ANOVA ( $p < 0.05$ ), *post-hoc t*-tests were used to determine pairwise difference ( $p < 0.05$ ). Results are shown uncorrected for multiple comparisons.

*State analysis*

An additional in-depth analysis was performed to shed light on the functional differences among the three groups. The K-means clustering algorithm was used to cluster the set of all distance matrices over all window slices of all the subjects into a number of  $k$  clusters (Schwarz, 1978). The K-means clustering algorithm identifies the most typical functional states by trying to minimize within cluster variances. The distance between two states was computed using the L1 norm. The K-means algorithm was randomly initialized, and run 500 epochs to escape local minima. We used the Bayesian Information Criterion (BIC) (Schwarz, 1978) to determine the value of  $k$ , the number of clusters. The BIC measure assumes a likelihood model, which can be constructed by viewing the k-means clustering as a Gaussian mixture model.

BIC is defined in Equation (7):

$$BIC = -2 \ln p(X|\Theta, M) + k(\ln n - \ln 2 \pi) \quad (7)$$

Where  $p(X|\Theta, M)$  is the marginal likelihood function given the model  $M$  and the parameter  $\Theta$ . The parameter,  $k$ , is the number of free parameters to be estimated, and  $n$  is the number of data points included in the dataset,  $X$  (Kass and

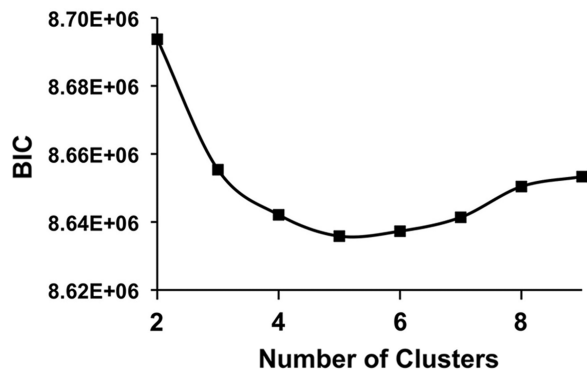


**FIG. 3.** BIC Scores for K-means Clustering. BIC scores with various numbers of clusters,  $k$ . The  $k$  with the lowest BIC is most preferable. BIC, Bayesian Information Criterion.

Raftery, 1995). A value of 5 for  $k$  for our dataset was chosen (Fig. 3) using the lowest BIC value for  $k$  ranging from 2 to 15. Once the five clusters were identified, the centroid of each functional state was determined.

The centroid states were used to label all the other states (i.e., distance matrices) based on their memberships in the  $k$ -means clustering. The individual functional activities can be described as a temporal transition between the centroid states. The three population groups may not spend an equal amount of time in any given state. We captured the characteristics of each state using the average connectivity strength, which is inversely proportional to the mean of global connection distance. The longer the functional distance, the more loosely functionally connected the brain is. In addition, the average SP of the global functional network and average weights of the MST of the global functional network were determined for each state.

## Results

The methodology described was applied to the resting state fMRI data on all participants including controls, PCS+ patients, and PCS- patients. Demographics for participants are shown in Table 1.

### Global functional connectivity

The differences in global functional connectivity among the three groups were analyzed by constructing a series of such networks using a moving time window for each subject as described in the previous section. Each series of networks produced a series of measurements  $Z_{s,1}, \dots, Z_{s,n \text{ windows}}$ , for subject,  $s$ , one for each time segment. The static average scores for the selected network properties (CC, SP, and MST) for each group are shown in Figure 4 and Table 2. The dynamic average scores are shown in Figure 5 and Table 3. A detailed comparison of the three subgroups including their network measurements, and results of the statistical analysis are summarized in Supplementary Tables S5 and S6.

Both static and dynamic methods uncovered differences of global functional networks between the PCS+ patients and the other two groups, PCS- and healthy controls (HC). Based on the results of the ANOVA, we observed a significant group differences in the static MST ( $p=0.017$ ). *Post-hoc*

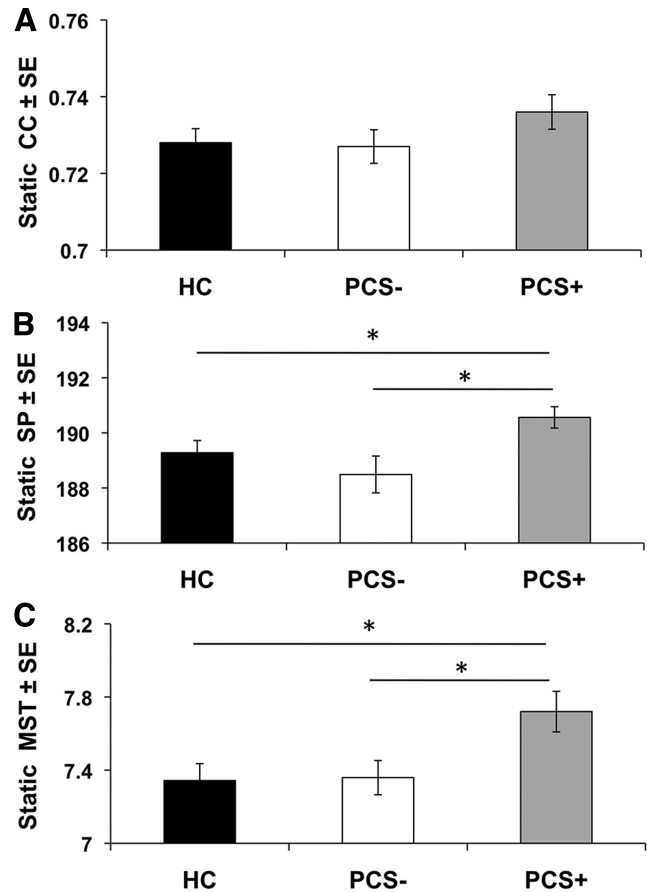


**FIG. 4.** Average static measurements of global network properties for the HC ( $n=30$ ), PCS+ ( $n=24$ ), and PCS- ( $n=23$ ) sub-groups. (A) Static average clustering coefficient (CC), (B) Static average shortest path (SP), (C) Static average weight of the minimum spanning trees (MST). \* $p < 0.05$  based on *post-hoc t*-tests. HC, healthy controls; PCS, post-concussion syndrome; PCS+, patients with PCS; PCS-, patients without PCS; SE, standard error.

*t*-tests revealed that PCS+ patients have larger MST compared to both the HC population ( $p=0.014$ ) and the PCS- patients ( $p=0.019$ ). In addition, we observed significant group differences in the static SP ( $p=0.026$ ). *Post-hoc t*-tests revealed that the PCS+ patients have larger SP compared to both the HC population ( $p=0.037$ ) and PCS- patients ( $p=0.013$ ). No differences were noted among the three groups in the static CC ( $p=0.291$ ) (Fig. 4). On the other hand, the dynamic analysis demonstrated significant group differences in the dynamic CC ( $p=0.033$ ) and dynamic SP ( $p=0.010$ ) (Fig. 5). *Post hoc t*-tests revealed that PCS+ patients have slower dynamic changes in CC ( $p=0.030$ ) and SP ( $p=0.016$ ) compared to the control population. Moreover, PCS+ patients also had slower changes occurring compared to PCS- patients in the dynamic SP ( $p=0.011$ ) and CC ( $p=0.003$ ). No differences in dynamic state of MST were noted between the three groups ( $p=0.207$ ).

### Preliminary sub-networks functional connectivity analysis

Studying the possible existence of statistical group differences within sub-networks can provide valuable insights into which sub-networks contribute to the differences noted in the whole-brain functional communication and also which sub-

TABLE 2. WHOLE BRAIN STATIC CONNECTIVITY RESULTS

	ANOVA		Mean ± STD			t-Test p-value		
	F	p-Value	HC	PCS+	PCS-	HC vs. PCS+	HC vs. PCS-	PCS+ vs. PCS-
CC	1.256	0.291	0.723 ± 0.020	0.736 ± 0.022	0.727 ± 0.021	NA	NA	NA
SP	3.833	<b>0.026</b>	189.280 ± 2.426	190.563 ± 1.902	188.490 ± 3.206	<b>0.037</b>	0.340	<b>0.013</b>
MST	4.315	<b>0.017</b>	7.343 ± 0.506	7.720 ± 0.543	7.359 ± 0.449	<b>0.014</b>	0.909	<b>0.019</b>

Bold indicates  $p < 0.05$ .

CC, clustering coefficient; MST, minimum spanning trees; SP, shortest path; STD, standard deviation.

networks may be most impacted by mTBI in a resting brain. In this preliminary analysis, we separately examined the set of time series belonging to each sub-network using the same graph-theoretic methodology including SP, CC, and MST. The sub-networks of interest include the visual network, cognitive control network, DMN, auditory network, cerebellar network, sub-cortical network, and sensorimotor network. The sub-network measurements along a sliding window were summarized to a single measure, using either the static or the dynamic method defined in Equations (5) and (6).

The results of the auditory sub-network are summarized in Supplementary Tables S5 and S6. While no group differences were noted in dynamic functional connectivity for the CC, SP or MST, significant group differences were noted in the static SP ( $p = 0.023$ ) (Supplementary Fig. S1). *Post hoc* t-tests reveal that these group differences are driven by a decreased connectivity in the PCS+ patients compared to the PCS- patients in the static SP ( $p = 0.011$ ). In addition, group differences were noted in the static CC for the visual network ( $p = 0.013$ ). *Post-hoc* t-tests reveal that PCS+ patients have increased static CC compared to the controls ( $p = 0.009$ ).

Based on the results of the ANOVAs for the other sub-networks, there was no evidence of significant group differences for the cognitive control network, DMN, sub-cortical network, sensorimotor network, or cerebellar network.

State analysis

To compare the different states, the connectivity strengths were computed and ranked with 1 being the strongest and 5 being the weakest for each of the five states. Note that the connectivity ranking of 1 indicates the smallest distances and hence stronger functional connection. The ranks and the amount of time each of our populations remained in a state are summarized in Table 4. The average percent of time in each state for each of the three groups is illustrated in Figure 6A. Connectivity matrices representing each state can be visualized as illustrated in Figure 6B. Group wise differences in average connectivity within each state can be visualized as illustrated in Supplementary Figure S2. It is apparent that PCS+ subjects spend very different amounts of time in most of the states compared to both the controls and PCS-. In particular, the PCS+ subjects spend 34.63% of their time in State 2, the state in which the other two cohorts only spent half that time.

Discussion

This study is one of the first to apply a combination of dynamic functional analysis and graph theoretic algorithms to distinguish mTBI from control participants. We demonstrate unique alterations in static and dynamic functional connectivity at the acute stage of injury in mTBI patients who will later suffer from persistent PCS when compared to both control participants and those mTBI patients who make a more complete recovery. Based on our findings, we arrive at three main conclusions. First, our findings regarding altered static functional connectivity are consistent with previous reports suggesting that in the acute stage of injury, functional communication is disrupted on both a global scale as well as providing preliminary evidence of disruptions within individual

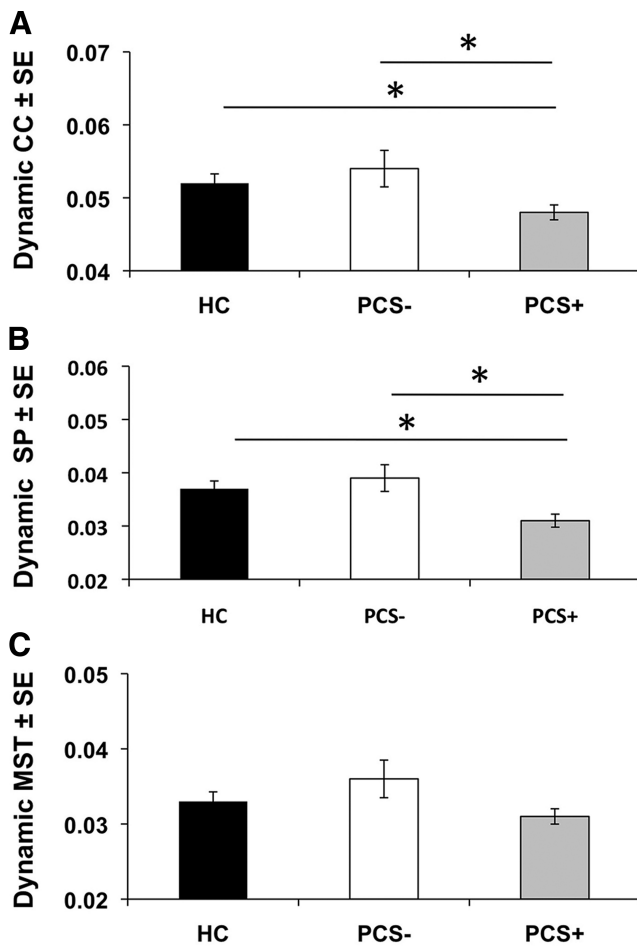


FIG. 5. Average dynamic measurements of global network properties for the HC ( $n = 30$ ), PCS+ ( $n = 24$ ), and PCS- ( $n = 23$ ) sub-groups. (A) Static average clustering coefficient (CC), (B) Static average shortest path (SP), (C) Static average weight of the minimum spanning trees (MST).  $*p < 0.05$  based on *post-hoc* t-tests. SE, standard error.

TABLE 3. WHOLE BRAIN DYNAMIC ANALYSIS RESULTS: WINDOW SIZE 6, STEP LENGTH 5

	ANOVA		Mean $\pm$ STD			t-Test p-value		
	F	p-Value	HC	PCS+	PCS-	HC vs. PCS+	HC vs. PCS-	PCS+ vs. PCS-
CC	3.553	<b>0.033</b>	0.052 $\pm$ 0.007	0.048 $\pm$ 0.005	0.054 $\pm$ 0.009	<b>0.030</b>	0.442	<b>0.016</b>
SP	4.878	<b>0.010</b>	0.037 $\pm$ 0.008	0.031 $\pm$ 0.006	0.039 $\pm$ 0.012	<b>0.003</b>	0.601	<b>0.011</b>
MST	1.606	0.207	0.033 $\pm$ 0.007	0.031 $\pm$ 0.005	0.036 $\pm$ 0.012	NA	NA	NA

Bold indicates  $p < 0.05$ .

CC, clustering coefficient; MST, minimum spanning trees; SP, shortest path; STD, standard deviation.

sub-networks. Second, the results show that the dynamics of functional communication are uniquely changed in mTBI patients who have postconcussive symptoms persisting into the chronic stage following injury. These changes in network dynamics are seen on a global level suggesting that damage to the overall communication across various functional networks may be associated with chronic symptoms. Finally, our results show that mTBI patients with poor outcomes spend a different amount of time in certain neural network configurations compared to the control subjects and the patients without persistent symptoms, providing further insights into possible neural contributions to chronic symptoms. These conclusions are further discussed in the following sections.

#### Alterations in static functional connectivity

Static functional connectivity analysis uncovered differences between PCS+ patients and both control subjects and PCS- patients. Figure 4 and the corresponding Table 2 show in detail how each group is quantitatively different from each other. Specifically, PCS+ patients have larger static MST and SP compared to both the controls and PCS- patients. Static MST and SP are closely related to the broadcast cost of a network; therefore, large static MST and SP suggest a costly, less efficient communication within the network. These results suggest that there is greater disruption in the functional communication both within and between various neural networks in mTBI patients with persistent symptoms compared to those without chronic symptoms.

The implications of these findings are two-fold. To our knowledge this is the first time that global functional connectivity measures have shown differences in mTBI patients based on self-reported symptomology. There is great variability in the literature regarding functional connectivity changes following mTBI within and between various networks as well as globally. This may be related to the fact that studies often included both patients with and without persistent symptoms, and the fact that analysis was not per-

formed on these studies based on long term outcomes, rather the analysis was based only on a single stage of imaging (Iraji et al., 2015; Johnson et al., 2012; Sours et al., 2013; Tang et al., 2011; Vergara, 2017b; Zhou et al., 2012). Our findings are further strengthened by the fact that connectivity differences were not observed between the patients who make a more complete recovery compared to the control group at this acute time point, suggesting either a protective mechanism within these patients or a difference in the initial injury sequelae. As the field continues to move toward the identification, and targeted treatment, of sub-categories of TBI patients, additional research into the predictive value of functional and structural neuroimaging modalities is needed to guide these classifications.

#### Alterations in dynamic functional connectivity

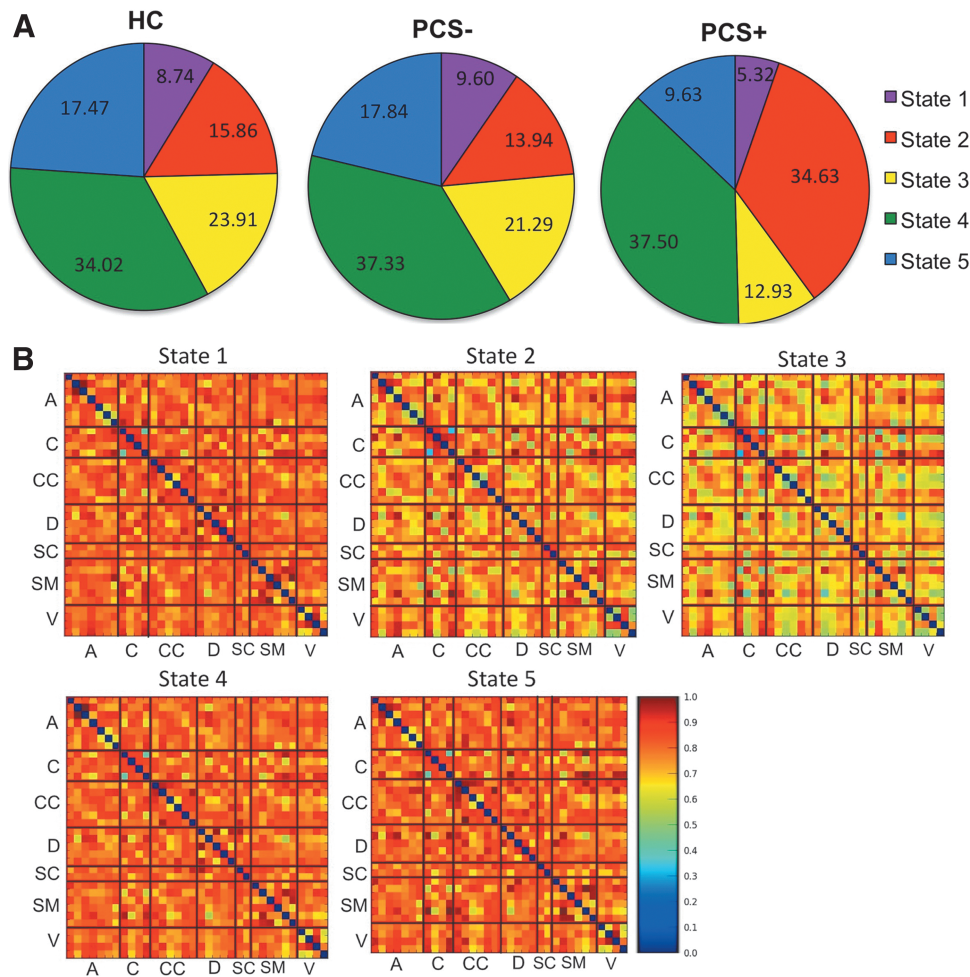
On a global scale, our results demonstrate that mTBI patients with chronic symptoms have slower dynamic functional connectivity as evidenced by a reduced dynamic SP and dynamic CC compared to the control group and PCS- patients (Fig. 5 and Table 3). While the influence of mTBI on dynamic functional connectivity has not been as extensively studied as static functional connectivity measures following mTBI, our results provide initial evidence that functional dynamics of PCS+ patients change at a slower rate than that of the controls and PCS- patients. On the other hand, in a recent report, group differences in dynamic connectivity measures between mTBI patients and controls were not observed after statistically controlling for multiple comparisons (Mayer et al., 2015). Specifically, the article focused on group comparisons within the DMN and sub-cortical structures using a dynamic sliding window method. Their findings were based on measures of static or dynamic connectivity within specific networks. Although their methodology was similar to ours and was based on the analysis of dynamic connectivity at a single time point following injury in the semi-acute stage (within 21 days compared to within 10 days within our population),

TABLE 4. STATE ANALYSIS

	Connectivity length	Average MST	Average SP	HC (%)	PCS+ (%)	PCS- (%)
State-1	36.16 (5)	1.57	37.25	8.74	5.32	9.60
State-2	32.18 (4)	1.53	33.15	15.86	34.63	13.94
State-3	25.66 (1)	1.21	26.44	17.47	9.63	17.84
State-4	29.10 (2)	1.37	29.98	34.02	37.50	37.33
State-5	31.41 (3)	1.34	32.36	23.91	12.93	21.29

Characteristics of each state and the time spent in each state for HC and mTBI PCS+ and PCS-.

Values in parentheses indicate the rank of the connectivity strengths with 1 being the strongest and 5 being the weakest. mTBI, mild traumatic brain injury.



**FIG. 6.** Results of the state analysis. **(A)** Percent of time that the HC ( $n=30$ ), mTBI PCS+ ( $n=24$ ), and mTBI PCS- ( $n=23$ ) spend in each of the five states. Characteristics of each state are shown in Table 4. **(B)** Average connectivity matrices for each of the five states. A, Auditory network; C, cerebellar network; CC, cognitive control network, D, default mode network; mTBI, mild traumatic brain injury, SC, subcortical network, SM, sensory motor network, V, visual network.

their analysis was focused on group differences and not long-term outcomes which may explain the differences in findings. However, this group recently, reanalyzed their data using different methodology and noted increased dynamic functional network connectivity between cerebellum and sensorimotor networks within specific connectivity states (Vergara et al., 2018). This result further highlights the potential impact that different methods have on reported group differences and remains a limitation within this upcoming field.

The differentiation of mTBI patients according to their recovery 6 months after the injury is a unique contribution that our study brings to the current literature. The reduced ability to efficiently transition between various neural network configurations may make an individual more susceptible to poor recovery leading to long-term persistent symptoms. Other predisposing factors might further exacerbate the extent of mTBI in patients with pre-existing psychiatric or substance abuse problems, poor general health, concurrent orthopedic injuries, or comorbid problems (e.g., chronic pain, depression, and increased life stress such as unemployment, and protracted litigation) (Isometsa, 2014; Osborn et al., 2014; Rees, 2003). These pre-existing conditions along with the injury are known to alter physiological factors such as cerebral blood flow (Ge et al., 2009; Kim et al., 2010, 2012), which ultimately may change the BOLD signal. While groups have consistently noted reduced resting state functional connectivity following mTBI (Johnson et al., 2012; Mayer et al.,

2011; Zhou et al., 2012), these findings, and the ones presented here, must be taken in context of the possible confounds of altered perfusion or vascular damage.

While long-term recovery is influenced by numerous factors, the ability to use clinically feasible imaging techniques to predict which patients will likely suffer from chronic symptoms is of great interest to both clinicians and researchers. Since the majority of mTBI cases are rarely followed up clinically, the ability to foresee patient outcomes would allow for increased monitoring of patients and the potential for early interventions to ameliorate symptoms.

#### Alterations in sub-networks

In our preliminary analysis of altered dynamic and static functional connectivity within individual neural networks, we found the greatest functional changes within the auditory and visual networks. mTBI patients with persistent symptoms have greater static SP within the auditory sub-network compared to mTBI patients without chronic symptoms as well as greater CC within the visual network compared to the control population. While early research has shown that disrupted network connectivity exists across certain networks including the DMN (Johnson et al., 2012; Mayer et al., 2011; Sours et al., 2015a; Zhou et al., 2012), the resting functional connectivity within the auditory and visual networks has rarely been investigated in the acute stages of mTBI. However, the altered

communication within networks that process sensory inputs in the acute stage of injury may influence the strong prevalence of somatic symptoms immediately following injury (blurry vision, difficulty in balancing and orientation, and ringing in the ear) (Dischinger et al., 2009). Previous research using task-based fMRI has demonstrated that mTBI patients exhibit a hypo-activation of multiple cortical and sub-cortical regions involved in auditory processing and attention during an auditory reorienting paradigm (Mayer et al., 2009). Furthermore, it has been shown that TBI patients have reduced processing speed and greater variability in reaction time following injury (Hillary et al., 2010; Johansson et al., 2009), which may suggest that visual and/or auditory processing is impaired in these patients. mTBI patients who acutely experience greater auditory symptoms (tinnitus or sensitivity to noise) or greater visual symptoms (sensitivity to light, blurry vision), may be more likely to have persistent symptoms. Although Vergara et al. (2018) did not report differences in dynamic connectivity within the auditory or visual networks in the semi-acute stage, they did report differences between the cerebellum and sensorimotor networks. The differences between their findings and ours may be due to differences in methodology or time since injury; however, this does provide additional evidence that future work investigating the association between sensory processing and patient outcome in a larger population is needed to validate these conjectures.

The DMN, which is one of the most frequently investigated resting state networks, has been consistently shown to be disrupted following mTBI (Iraji et al., 2015; Johnson et al., 2012; Mayer et al., 2011; Sours et al., 2013, 2015a; Zhou et al., 2012). For instance, Zhou et al., found substantial reductions of connectivity in the posterior cingulate cortex and parietal regions and increased connectivity around the medial prefrontal cortex in patients with mTBI (Zhou et al., 2012). This reduced posterior connectivity was shown to be positively associated with neurocognitive dysfunction, while the increased frontal connectivity was shown to be negatively correlated with increased symptoms. Their work suggests the existence of brain alterations in resting state DMN in the sub-acute phase of mTBI. However, in the present study we did not find evidence of group differences in static or dynamic functional connectivity within the DMN among our three cohorts. While our results failed to replicate the findings of Zhou et al., this might reflect the heterogeneous nature of mTBI itself. Alternatively it is possible that our specific methodology may not have been sensitive enough to detect subtle changes within the DMN. However, in this analysis we limited our attention to alterations in static and dynamic connectivity changes *within* each sub-network, which does not take into account mTBI induced changes *between* various sub-networks that previously have been shown to be altered following mTBI (Mayer et al., 2011; Sours et al., 2013).

#### State analysis

In Allen et al. (2014) and Damaraju et al. (2014), the k-means clustering technique is applied to the distance matrices computed over each time window to identify a small number of functional connectivity states. These functional connectivity states are analogous to the EEG micro-states, short periods during which scalp topography remains quasi-stable (Lehmann, 1990). The states are identified as

the centroids of the clusters generated by the k-means clustering algorithm applied to the distance matrices calculated within each time window. A centroid of a cluster is a matrix such that each entry is the mean of the corresponding entries in the matrices in the cluster. These distance matrices reflect the most typical and common states the brain traverses as part of various cognitive or emotional states. The characteristics of each brain state and the distribution of the time each group spends in each state, together with the variations in static and dynamic connectivity characteristics, can provide insights into the differences among the three groups.

For efficient behavior, the brain must be able to fluidly transition between different network configurations based on existing external demands or emotional needs. These different network configurations have variable network properties and can likely be attributed to different cognitive, attentional, or emotional states. The results of the state analysis demonstrate that PCS+ patients spend a strikingly different amount of time in the five major brain states compared to both the PCS- patients and control population, who spend roughly identical amounts of time in each of the five brain states.

For instance, while all three groups spend roughly the same amount of time in state 4 which is characterized by average strength of connectivity and average network measures, PCS+ patient spend significantly less time in state 3 compared to the two other groups (10.0% compared to 18.0% and 17.4% respectively). While state 3 shows average connectivity strength, this state has the smallest SP and MST, which reflects a high efficiency in transmission between the regions. This suggests that PCS+ patients spend less time in a highly efficient network configuration. On the contrary, state 1 displays a decreased link efficiency and high tendency for local cliqueness. PCS+ patients also spend roughly half as much time in state 1 compared to the PCS- and control groups suggesting that mTBI patients who develop persistent symptoms spend less time in a highly modular brain state.

On the other hand, PCS+ patients remain in state 2 for the majority of the time, nearly twice as much as the control and PCS- groups. State 2 is characterized by large MST and SP but low strength of functional connectivity. Together they indicate disruption of the small world topology, which is again suggestive of a less efficient network configuration. Taken together, the reduced amount of time spent in state 1 and state 5 may suggest why PCS+ patients have reduced strength of connectivity and slower dynamic functional connectivity because of the reduced rate of transition between the major neural network configurations. The fact that PCS+ patients have two major states, state 2 and state 4, may contribute to the fact that PCS+ patients demonstrate reduced functional dynamics. Our findings are further supported by recent work demonstrating that network state occupancy rates for semi-acute mTBI patients differ from controls (Vergara et al., 2017b) as well as fewer state transitions in a chronic severe TBI population compared to controls (Gilbert et al., 2018). However, the authors provide evidence that the results were dependent on the specific preprocessing pipelines used suggesting a potential limitation to the findings outlined in this analysis.

#### Use of L1 norm

In this work, the L1 norm is used instead of correlation measures to quantify the distance or dissimilarity of fMRI

time series. We choose this metric because the L1 norm is widely regarded as a reliable distance metric for time series, and is more appropriate than similarity measures for our graph-theoretic metrics. Moreover, it is often utilized in fMRI literature as regularization to capture the aspect of dissimilarity between time series (Ryali et al., 2010, 2012). The association between L1 norm and Pearson correlation has been studied in a high performance computing setting (Minati et al., 2014) and it was concluded that L1 norm should be considered as a replacement for correlation in dense resting-state functional analysis.

### Limitations

While our results represent novel evidence that mTBI patients with persistent symptoms in the chronic stages of injury have altered functional dynamics in the acute stage of injury, our findings must be taken in the context of the limitations of the current study. In this preliminary investigation of altered static and dynamic connectivity measures, we selected three graph theoretical measures based on a literature review. However, there remains an extensive list of other graph theoretic measures that would be worthwhile to investigate in the future. While the results appear to be quite robust when using the norm L1 in our case and no mitigation was necessary, it should be noted that L1-norm dissimilarity may suffer from artifact fluctuations due to the problem of windowing (e.g., selecting a shorter time period). In future work we plan to consider the possibility of artifacts in more depth and develop necessary adjustments to mitigate such artifacts (Leonardi and Van De Ville, 2015; Zalesky and Breakspear, 2015). An additional limitation of this study is the limited size of the mTBI population and that this population included individuals with variable injury mechanisms. Future work investigating the specific static and dynamic network disruptions associated with specific injury mechanisms is needed to further elucidate this question as well as determine the generalizability of this data to the larger TBI population.

### Conclusion

In conclusion, our findings suggest that on a global scale, mTBI patients who will develop persistent symptoms demonstrate slowed network dynamics and unique allocation of time to various brain states compared to control participants and mTBI patients who have a more complete recovery. In particular, mTBI patients with chronic symptoms demonstrate reduced small world connectedness, and are slower to transition between major network states compared to control subjects and patients without chronic symptoms. Our findings indicate that both static and dynamic functional analyses can provide powerful insights into the neural correlates of the brain associated with altered function in mTBI patients. Furthermore, these findings suggest the possibility of early diagnosis of those patients whose mTBI may result in a poor outcome. Future research exploring more advanced network properties is needed to more precisely define the unique contributions of different neural networks to the group differences reported in this study as well as aid in the neurological interpretation of these findings.

### Acknowledgments

We gratefully acknowledge funding provided by The University of Maryland/Powering the State through the Center for

Health-related Informatics and Bioimaging (CHIB) to R.P.G. and J.J. Support for this work was in part provided by the Department of Defense (W81XWH-08-1-0725, W81XWH-12-1-0098) and National Institutes of Health (1R01NS105503).

### Author Disclosure Statement

No competing financial interests exist.

### Supplementary Material

Supplementary Figure S1  
 Supplementary Figure S2  
 Supplementary Table S1  
 Supplementary Table S2  
 Supplementary Table S3  
 Supplementary Table S4  
 Supplementary Table S5  
 Supplementary Table S6

### References

- Allen EA, Damaraju E, Plis SM, Erhardt EB, Eichele T, Calhoun VD. 2014. Tracking whole-brain connectivity dynamics in the resting state. *Cereb Cortex* 24:663–676.
- Calhoun VD, Miller R, Pearson G, Adali T. 2014. The chronnectome: time-varying connectivity networks as the next frontier in fMRI data discovery. *Neuron* 84:262–274.
- Chang C, Glover GH. 2010. Time-frequency dynamics of resting-state brain connectivity measured with fMRI. *Neuroimage* 50:81–98.
- Cherkassky BV, Goldberg AV, Radzik T. 1996. Shortest paths algorithms: theory and experimental evaluation. *Math Program* 73:129–174.
- Cox RW. 1996. AFNI: software for analysis and visualization of functional magnetic resonance neuroimages. *Comput Biomed Res* 29:162–173.
- Damaraju E, Allen EA, Belger A, Ford JM, McEwen S, Mathalon DH, et al. 2014. Dynamic functional connectivity analysis reveals transient states of dysconnectivity in schizophrenia. *Neuroimage Clin* 5:298–308.
- Ding H, Trajcevski G, Scheuermann P, Wang X, Keogh E. 2008. Querying and mining of time series data: experimental comparison of representations and distance measures. *Proceedings VLDB Endowment* 1:1542–1552.
- Dischinger PC, Ryb GE, Kufera JA, Auman KM. 2009. Early predictors of postconcussive syndrome in a population of trauma patients with mild traumatic brain injury. *J Trauma* 66:289–296; discussion 296–297.
- Faul M, Xu L, Wald M, Coronado V. 2010. Traumatic Brain Injury in the United States: Emergency Department Visits, Hospitalizations, and Deaths. Atlanta, GA: Centers for Disease Control and Prevention.
- Ge Y, Patel MB, Chen Q, Grossman EJ, Zhang K, Miles L, et al. 2009. Assessment of thalamic perfusion in patients with mild traumatic brain injury by true FISP arterial spin labelling MR imaging at 3T. *Brain Inj* 23:666–674.
- Gilbert N, Bernier RA, Calhoun VD, Brenner E, Grossner E, Rajtmajer SM, et al. (2018) Diminished neural network dynamics after moderate and severe traumatic brain injury. *PLoS One* 13:e0197419.
- Hillary FG, Genova HM, Medaglia JD, Fitzpatrick NM, Chiou KS, Wardecker BM, et al. 2010. The nature of processing speed deficits in traumatic brain injury: is less brain more? *Brain Imaging Behav* 4:141–154.

- Hoerl AE, Kennard RW. 1970. Ridge regression: biased estimation for nonorthogonal problems. *Technometrics* 12: 55–67.
- Hutchison RM, Womelsdorf T, Allen EA, Bandettini PA, Calhoun VD, Corbetta M, et al. 2013. Dynamic functional connectivity: promise, issues, and interpretations. *Neuroimage* 80:360–378.
- Hyvarinen A. 1999. Fast ICA for noisy data using Gaussian moments. In: *Proceedings of the 1999 IEEE International Symposium on Circuits and Systems VLSI (Cat. No.99CH36349)*, Orlando, FL, 1999, pp. 57–61.
- Iraji A, Benson RR, Welch RD, O’Neil BJ, Woodard JL, Ayaz SI, et al. 2015. Resting state functional connectivity in mild traumatic brain injury at the acute stage: independent component and seed based analyses. *J Neurotrauma* 32:1031–1045.
- Isometsa E. 2014. Suicidal behaviour in mood disorders—who, when, and why? *Can J Psychiatry* 59:120–130.
- Johansson B, Berglund P, Ronnback L. 2009. Mental fatigue and impaired information processing after mild and moderate traumatic brain injury. *Brain Inj* 23:1027–1040.
- Johnson B, Zhang K, Gay M, Horovitz S, Hallett M, Sebastianelli W, Slobounov S. 2012. Alteration of brain default network in subacute phase of injury in concussed individuals: resting-state fMRI study. *Neuroimage* 59:511–518.
- Kass RE, Raftery AE. 1995. Bayes factors. *J Am Stat Assoc* 90: 773–795.
- Kim J, Whyte J, Patel S, Avants B, Europa E, Wang J, et al. 2010. Resting cerebral blood flow alterations in chronic traumatic brain injury: an arterial spin labeling perfusion fMRI study. *J Neurotrauma* 27:1399–1411.
- Kim J, Whyte J, Patel S, Europa E, Slattery J, Coslett HB, Detre JA. 2012. A perfusion fMRI study of the neural correlates of sustained-attention and working-memory deficits in chronic traumatic brain injury. *Neurorehabil Neural Repair* 26:870–880.
- King NS, Crawford S, Wenden FJ, Moss NE, Wade DT. 1995. The Rivermead Post Concussion Symptoms Questionnaire: a measure of symptoms commonly experienced after head injury and its reliability. *J Neurol* 242:587–592.
- Lehmann D. 1990. Brain electric microstates and cognition; the atoms of thought. In: Roy John E (ed.) *Machinery of the Mind*. Boston, MA: Birkhuser; pp. 209–224.
- Leonardi N, Van De Ville D. 2015. On spurious and real fluctuations of dynamic functional connectivity during rest. *Neuroimage* 104:430–436.
- Mayer AR, Ling JM, Allen EA, Klimaj SD, Yeo RA, Hanlon FM. 2015. Static and dynamic intrinsic connectivity following mild traumatic brain injury. *J Neurotrauma* 32:1046–1055.
- Mayer AR, Mannell MV, Ling J, Elgie R, Gasparovic C, Phillips JP, et al. 2009. Auditory orienting and inhibition of return in mild traumatic brain injury: a fMRI study. *Hum Brain Mapp* 30:4152–4166.
- Mayer AR, Mannell MV, Ling J, Gasparovic C, Yeo RA. 2011. Functional connectivity in mild traumatic brain injury. *Hum Brain Mapp* 32:1825–1835.
- McMahon P, Hricik A, Yue JK, Puccio AM, Inoue T, Lingsma HF, et al. 2014. Symptomatology and functional outcome in mild traumatic brain injury: results from the prospective TRACK-TBI study. *J Neurotrauma* 31:26–33.
- Minati L, Zaca D, D’Incerti L, Jovicich J. 2014. Fast computation of voxel-level brain connectivity maps from resting-state functional MRI using l(1)-norm as approximation of Pearson’s temporal correlation: proof-of-concept and example vector hardware implementation. *Med Eng Phys* 36: 1212–1217.
- Osborn AJ, Mathias JL, Fairweather-Schmidt AK. 2014. Depression following adult, non-penetrating traumatic brain injury: a meta-analysis examining methodological variables and sample characteristics. *Neurosci Biobehav Rev* 47C:1–15.
- Pedregosa F, Varoquaux G, Gramfort A, Michel V, Thirion B, Grisel O, et al. 2011. Scikit-learn: machine learning in python. *J Mach Learn Res* 12:2825–2830.
- Pettie S, Ramachandran V. 2002. An optimal minimum spanning tree algorithm. *J Assoc Comput Mach* 49:16–34.
- Rees PM. 2003. Contemporary issues in mild traumatic brain injury. *Arch Phys Med Rehabil* 84:1885–1894.
- Ryali S, Chen T, Supekar K, Menon V. 2012. Estimation of functional connectivity in fMRI data using stability selection-based sparse partial correlation with elastic net penalty. *Neuroimage* 59:3852–3861.
- Ryali S, Supekar K, Abrams DA, Menon V. 2010. Sparse logistic regression for whole-brain classification of fMRI data. *Neuroimage* 51:752–764.
- Sair HI, Yahyavi-Firouz-Abadi N, Calhoun VD, Airan RD, Agarwal S, Intrapiromkul J, et al. 2016. Presurgical brain mapping of the language network in patients with brain tumors using resting-state fMRI: comparison with task fMRI. *Hum Brain Mapp* 37:913–923.
- Saramaki J, Kivela M, Onnela JP, Kaski K, Kertesz J. 2007. Generalizations of the clustering coefficient to weighted complex networks. *Phys Rev E Stat Nonlin Soft Matter Phys* 75:027105.
- Schwarz GE. 1978. Estimating the dimension of a model. *Ann Stat* 6:461–464.
- Sours C, Chen H, Roys S, Zhuo J, Varshney A, Gullapalli RP. 2015a. Investigation of multiple frequency ranges using discrete wavelet decomposition of resting state functional connectivity in mild traumatic brain injury patients. *Brain Connect* 5:442–450.
- Sours C, Rosenberg J, Kane R, Roys S, Zhuo J, Shanmuganathan K, Gullapalli RP. 2015b. Associations between interhemispheric functional connectivity and the Automated Neuropsychological Assessment Metrics (ANAM) in civilian mild TBI. *Brain Imaging Behav* 9:190–203.
- Sours C, Zhuo J, Janowich J, Aarabi B, Shanmuganathan K, Gullapalli RP. 2013. Default mode network interference in mild traumatic brain injury—a pilot resting state study. *Brain Res* 1537:201–215.
- SPM8. 2009. Statistical Parametric Mapping. Wellcome Department of Imaging Neuroscience, University College London, United Kingdom.
- Stevens MC, Lovejoy D, Kim J, Oakes H, Kureshi I, Witt ST. 2012. Multiple resting state network functional connectivity abnormalities in mild traumatic brain injury. *Brain Imaging Behav* 6:293–318.
- Talairach J, Tournoux P. 1988. *Co-planar Stereotaxic Atlas of the Human Brain*. New York, NY: Thieme.
- Tang L, Ge Y, Sodickson DK, Miles L, Zhou Y, Reaume J, Grossman RI. 2011. Thalamic resting-state functional networks: disruption in patients with mild traumatic brain injury. *Radiology* 260:831–840.
- Tie Y, Rigolo L, Norton IH, Huang RY, Wu W, Orringer D, et al. 2014. Defining language networks from resting-state fMRI for surgical planning—a feasibility study. *Hum Brain Mapp* 35:1018–1030.
- van den Heuvel MP, Mandl RC, Kahn RS, Hulshoff Pol HE. 2009. Functionally linked resting-state networks reflect the

- underlying structural connectivity architecture of the human brain. *Hum Brain Mapp* 30:3127–3141.
- Varoquaux G, Keller M, Poline J, Ciuciu P, Thirion B. 2010a. ICA-based sparse features recovery from fMRI datasets. In: *Proceedings of 2010 IEEE International Symposium on Biomedical Imaging*. Rotterdam, Netherlands, 2010. pp. 1177.
- Varoquaux G, Sadaghiani S, Pinel P, Kleinschmidt A, Poline JB, Thirion B. 2010b. A group model for stable multi-subject ICA on fMRI datasets. *Neuroimage* 51:288–299.
- Vergara VM, Mayer AR, Damaraju E, Calhoun VD. 2017a. The effect of preprocessing in dynamic functional network connectivity used to classify mild traumatic brain injury. *Brain Behav* 7:e000809.
- Vergara VM, Mayer AR, Damaraju E, Kiehl KA, Calhoun V. 2017b. Detection of mild traumatic brain injury by machine learning classification using resting state functional network connectivity and fractional anisotropy. *J Neurotrauma* 34:1045–1053.
- Vergara VM, Mayer A, Kiehl KA, Calhoun VD. 2018. Dynamic functional network connectivity discriminates mild traumatic brain injury through machine learning. *Neuroimage Clin* 19:30–37.
- Watts DJ, Strogatz SH. 1998. Collective dynamics of ‘small-world’ networks. *Nature* 393:440–442.
- World Health Organization. 2010. *International Classification of Disease, 10th Review*. Geneva, Switzerland: World Health Organization.
- Zalesky A, Breakspear M. (2015). Towards a statistical test for functional connectivity dynamics. *Neuroimage* 114:466–470.
- Zhou Y, Milham MP, Lui YW, Miles L, Reaume J, Sodickson DK, et al. 2012. Default-mode network disruption in mild traumatic brain injury. *Radiology* 265:882–892.

Address correspondence to:

*Rao P. Gullapalli*

*Department of Diagnostic Radiology and Nuclear Medicine*

*University of Maryland School of Medicine*

*22 South Greene Street*

*Baltimore, MD 21201*

*E-mail: rgullapalli@umm.edu*

*Joseph JaJa*

*Department of Electrical and Computer Engineering*

*University of Maryland Institute for Advanced Computer*

*Services (UMIACS)*

*3433 A.V. Williams Bldg*

*University of Maryland*

*College Park, MD 20742*

*E-mail: josephj@umd.edu*